



ORIGINAL ARTICLE

Achillea biebersteinii-Mediated Gold Nanoparticles on Oocyte Gene Expression and Follicular Development in Mice

Mohammadreza Abdollahi^{1,2#} , Mohammad Zangoeei^{3#} , Parishad Ghorbani⁴ , Reihaneh Alsadat Mahmoudian^{5,6} , Atena Mansouri^{7*} 

1. Department of Anatomy, Faculty of Medicine, Birjand University of Medical Sciences, Birjand, Iran.
2. Innovated Medical Research Center & Department of Immunology, Mashhad Branch, Islamic Azad University, Mashhad, Iran.
3. Department of Nursing, Qaen School of Medical Sciences, Geriatric Health Research Center, Birjand University of Medical Sciences, Birjand, Iran.
4. Department of Biology, Faculty of Sciences, Ferdowsi University of Mashhad, Mashhad, Iran.
5. Cancer research Center, Mashhad University of Medical Sciences, Mashhad, Iran
6. Metabolic Syndrome Research Center, Mashhad University of Medical Sciences, Mashhad, Iran.
7. Cellular and Molecular Research Center, Birjand University of Medical Sciences, Birjand, Iran.

ARTICLE INFO

Received: 2025/04/12

Revised: 2025/07/26

Accepted: 2025/10/1

These authors are Co-First authors

*Corresponding:

Nafiseh Mortazavi

Address:

Cellular and Molecular
Research Center, Birjand
University of Medical Sciences,
Birjand, Iran

E-mail:

mansouri_atena@yahoo.com

ABSTRACT

This study investigated the effects of chemically synthesized gold nanoparticles (GNPs) and green gold nanoparticles (gGNPs) derived from *Achillea biebersteinii* extract on antrum diameter and the expression of genes associated with follicular development in NMRI mice. Female mice were treated with GNPs and gGNPs at concentrations of 10, 50, and 100 µg/mL. Antrum diameter in ovarian follicles was measured using ImageJ software. Gene expression levels of BMP-15, GDF-9, SOD, and GPx were quantified via real-time PCR. Treatment with gGNPs at 100 µg/mL significantly increased the antrum diameter of secondary follicles compared to GNPs ($p \leq 0.05$), while no significant changes were observed in grafted follicles. A dose-dependent upregulation of BMP-15, GDF-9, GPx, and SOD was observed in both GNP and gGNP groups, with gGNPs eliciting stronger effects across all genes ($p \leq 0.05$). The findings suggest that *A. biebersteinii*-mediated green synthesis enhances the biological activity of GNPs, particularly in promoting follicular development and antioxidant gene expression. Although mechanistic pathways were not explored in this study, future research should address these gaps and evaluate long-term safety and therapeutic potential.

Keywords: Gold Nanoparticles, *Achillea biebersteinii*, Expression, Gene, Antrum

Cite this article: Abdollahi M, et al. *Achillea biebersteinii*-Mediated Gold Nanoparticles on Oocyte Gene Expression and Follicular Development in Mice. International Journal of Molecular and Cellular Medicine. 2025; 14 (4):1072-1083. DOI: 10.22088/IJMCM.BUMS.14.4.1072



© The Author(s).

Publisher: Babol University of Medical Sciences

This work is published as an open access article distributed under the terms of the Creative Commons Attribution 4.0 License (<http://creativecommons.org/licenses/by-nc/4>). Non-commercial uses of the work are permitted, provided the original work is properly cited.

Introduction

Studies have shown that growth factors essential for follicular development are secreted by both oocytes and somatic cells. Among the members of the Transforming Growth Factor Beta (TGF- β) superfamily, Bone Morphogenetic Protein 15 (BMP15) and Growth Differentiation Factor 9 (GDF-9) play particularly important roles. These proteins are critical for granulosa cell differentiation and regulation of key cellular functions involved in folliculogenesis. Genetic abnormalities in BMP15 and GDF-9 have been linked to infertility, underscoring their crucial role in female reproductive health(1). The roles of BMP15 and GDF-9 have been extensively investigated using gene knockout and mutant models in mice, sheep, and humans. For example, female mice lacking the Gdf9 gene are infertile, highlighting its indispensable role(2). Moreover, double-mutant mice (Gdf9 $^{+/-}$ Bmp15 $^{-/-}$) exhibit more severe reproductive defects than Bmp15 $^{-/-}$ mice, indicating a synergistic effect of these genes(3). GDF-9 expression begins in oocytes during the primary stage and continues through ovulation, whereas BMP15 mRNA appears in oocytes from developing follicles at the primordial stage but not in dormant ones. Despite these differences, both proteins regulate folliculogenesis(4). In mice, BMP15 seems less essential for fertility, as Bmp15 $^{-/-}$ females are fertile with only a slight reduction in fecundity. In contrast, BMP15 is essential in sheep, where heterozygous mutations increase ovulation rates, demonstrating species-specific functional significance (5). Biologically active TGF- β superfamily members, including BMP15 and GDF-9, function as homo- or heterodimers and initiate downstream signaling by binding to transmembrane type I and type II serine/threonine kinase receptors(6) (7). In vitro studies show that BMP15 and GDF9 activate different pathways—SMAD1/5/8 for BMP15 and SMAD2/3 for GDF9(4, 8). The GDF9/BMP15 heterodimer phosphorylates SMAD2/3 via the BMPR2-ALK4/5/7-ALK6 receptor complex in granulosa cells, indicating potent regulatory functions in genes controlling cumulus expansion (9).

Oxidative stress is another key factor influencing follicular development. When reactive oxygen species (ROS) overwhelm the antioxidant defenses, follicle maturation, oocyte quality, and fertility can all be compromised (10). This process involves multiple

stages: primordial follicle recruitment, growth, dominant follicle selection, and ovulation. High metabolic activity during these stages increases vulnerability to ROS, potentially causing chromosomal abnormalities, DNA damage, and mitochondrial dysfunction, all of which impair oocyte quality and embryo development (11). Therefore, mitigating ROS-induced damage is a promising strategy to support follicular health. Endogenous antioxidant enzymes such as superoxide dismutase (SOD) and glutathione peroxidase (GPx), which are expressed in both oocytes and granulosa cells, play vital roles in maintaining redox balance during folliculogenesis(12). Disruptions in their expression can increase oxidative stress, impairing follicle development and fertility(13).

Over the past two decades, nanoparticle (NP) applications expanded significantly, especially in biomedical research. Numerous studies have investigated their effects on reproductive systems in animal models(14). Gold nanoparticles (GNPs) have shown great potential for drug delivery and cancer treatment due to their targeted cytotoxicity(15). One of the most efficient and eco-friendly methods for synthesizing GNPs is the use of plant extracts. These extracts, rich in antioxidants, can modify the biological behavior of GNPs during synthesis(16). Several studies have highlighted the biomedical applications of gold nanoparticles synthesized using plant extracts due to their enhanced biocompatibility and antioxidant potential (17). The genus *Achillea*, which includes more than 100 species—19 of which are native to Iran—is known for its antioxidant properties (18). Plants from this genus contain phenolic compounds that contribute to their strong free radical scavenging capabilities (19). There is a direct correlation between phenolic content and antioxidant potential(20).

Our previous *in vitro* research demonstrated that *Achillea biebersteinii* extract significantly enhanced preantral follicle (PF) growth by upregulating GDF-9, BMP-15, and GPx gene expression, while also reducing intracellular ROS levels. In contrast, chemically synthesized gold nanoparticles inhibited PF development, whereas green-synthesized GNPs (gGNPs) showed moderate biocompatibility due to surface modification by phytochemicals. These results suggested the potential protective and bioactive properties of AB extract and its nanoparticle formulation, laying the groundwork for the current *in vivo* investigation (21).

The current study was conducted to investigate the impact of *Achillea biebersteinii*-mediated green GNPs on the expression of folliculogenesis-related genes and antrum diameter in mice.

Methods

Preparation of Aqueous Extract from *Achillea biebersteinii*

Achillea biebersteinii was collected during the flowering season from natural habitats located in the northeastern region of Iran. The plant was authenticated by a botanist from the Faculty of Agriculture, Ferdowsi University of Mashhad. Although a formal herbarium code was not assigned, a voucher specimen was reviewed and confirmed by the expert and archived in the department for future reference. The aerial parts of the plant were thoroughly washed, air-dried in the shade at room temperature, and then powdered for extraction. The above-ground parts of *Achillea biebersteinii* were collected and dried at a temperature of 43°C. Once dried, the plant material was ground into a fine powder. 5-gram portion of the powdered material was combined with 100 mL of distilled deionized water (ddH₂O) and heated on a hot plate for 5 minutes with continuous stirring. Afterward, the mixture was filtered over Whatman No. 1 filter paper and stored at 4°C for future experiments. All experimental procedures were approved by Ferdowsi University of Mashhad with approval code: ۴۵۸۰۷

Gold nanoparticles (GNPs) with a diameter of 20 nm and a concentration of 400 µg/mL were employed in the experiment. Green gold nanoparticles (gGNPs) were prepared by combining the aqueous extract of *Achillea biebersteinii* with GNPs of the same size (20 nm) at a concentration of 300 µg/mL. Distilled water was used as the solvent for both the plant extract and the nanoparticle suspensions. These nanoparticles were sourced from the Mehregan Chem Group in Tehran, Iran, and were synthesized following the protocols outlined in our previous research (21).

Treatment of animals

In this study, 60 immature female NMRI mice, three weeks of age and weighing 10–20 grams, were used. The animals were provided by the animal facility of Ferdowsi University of Mashhad. The mice were selected at this prepubertal stage to allow for investigation of follicular development. They were

housed in standard laboratory cages with ad libitum access to food and water. Environmental conditions were maintained at a 12-hour light/dark cycle, 23±2°C temperature, and 50–68% relative humidity. The animals were allowed to acclimate for one week before the beginning of treatments. After acclimatization, they were randomly divided into ten groups (n = 6 per group). Control Group: No treatment was administered. AB Group: Received intraperitoneal injections of *Achillea biebersteinii* aqueous extract at doses of 10, 50, or 100 µg/mL daily for 10 days. GNP Group: Received intraperitoneal injections of GNPs at doses of 10, 50, or 100 µg/mL daily for 10 days. gGNP Group: Received intraperitoneal injections of gGNPs at doses of 10, 50, or 100 µg/mL daily for 10 days (۳۳).

Histological experiments

Sampling

In accord with the regulations of the Bioethics Committee (Birjand University of Medical Sciences), the animals were anesthetized using diethyl ether. The mouse's body was carefully opened using sterile scissors in a controlled environment. The ovaries were carefully detached and placed in physiological serum. The ovaries were immediately divided from the surrounding tissues under a stereomicroscope to ensure correct handling for the histotechnical procedures that followed.

Tissue processing

Tissue processing was performed using an Autotechnicon system. Initially, the specimens were immersed in 10% phosphate-buffered formalin for 48 hours. Dehydration was then achieved through a graded ethanol series (70%, 80%, 90%, 96%, and 100%). The clarification step involved immersing the samples in xylene placed in two containers for one hour. The samples were then molded into paraffin blocks using aluminum molds, and molten paraffin was dispensed through a paraffin dispenser. The resulting paraffin blocks contained the tissue samples. To prepare sections for microscopic examination, the paraffin blocks were cut into slices with a thickness of 5 micrometers using a microtome. The slices were treated with 10% ethyl alcohol to facilitate their placement on slides and were subjected to a 70°C water bath to eliminate any potential wrinkles. Hematoxylin and eosin (H&E) staining was then applied to the slides for microscopic examination.

Quantitative real-time PCR (qPCR)

In the present study, quantitative real-time PCR (qPCR) was performed to evaluate changes in gene expression. For RNA extraction, 100 mg of ovarian tissue samples (previously stored in RNAlater solution) were used. Total RNA was extracted using the TRIzol reagent kit (Parstous Biotechnology, Iran) following the manufacturer's protocol. The quantity and purity of the extracted RNA were assessed by NanoDrop spectrophotometry, and its integrity was confirmed by 1% agarose gel electrophoresis in TAE buffer. For cDNA synthesis, 1 µg (1000 ng) of total RNA was reversely-transcribed using the cDNA synthesis kit (Parstous Biotechnology, Iran) according to the supplied instructions. Gene-specific primers

were designed using AlleleID software, and their specificity and potential dimer formation were checked. Primer sequences and amplicon lengths are provided in Table 1. The qPCR reactions were carried out using the SYBR Green Master Mix kit (Parstous Biotechnology, Iran) on a real-time PCR system. Each reaction was performed in triplicate. The thermal cycling conditions included: Initial denaturation at 95°C for 15 seconds, Followed by 40 cycles of: Denaturation at 95°C for 15 seconds, Annealing at 62°C for 30 seconds, Extension at 72°C for 30 seconds. The GAPDH gene served as the internal reference. Gene expression levels were calculated using the $2^{-\Delta\Delta C_t}$ method, and no-template controls (NTCs) were included to verify the absence of contamination.

Table 1. Sequences of Primers used in this study

Gene	Forward primer	Reverse primer
BMP15	CAGTAAGGCCTCCCAGAGGT	AAGTTGATGGCGGTAACCA
GDF-9	TACCGTCCGGCTCTTCAGT	TAAACAGCAGGTCCACCATC
SOD	ACCATCCACTTCGAGCAGAA	AAAATGAGGTCCTGCACTGG
GPx	CATACCGGTTATGCGCTGGTA	CCTCATGTAAGACAGGATGTCCAT
GAPDH	AACTCCACTCTTCCACCTTCG	GTCCACCACCCTGTTG CTGTAG

Results

Gene expression analysis

Our research investigated the effects of *Achillea biebersteinii* (AB) extract and gold nanoparticles (GNPs) on gene expression related to follicular development in a mouse model. We observed significant alterations in the expression of BMP15, GDF-9, SOD, and GPx genes across various treatment groups, indicating that both AB extract and GNPs can modulate key aspects of ovarian function.

BMP15 Gene Expression

The expression of BMP-15 was upregulated in the gGNP 50 µg/mL and gGNP 100 µg/mL groups (fold change > 5 and ~3.4 respectively), compared to the control group. Notably, BMP-15 expression was markedly suppressed in the extract-only 50 µg/mL group (fold < 0.3), but elevated in GNP 10 µg/mL (fold ~2.8). These results indicate that green-synthesized gold nanoparticles potentiate the expression of BMP-15 more effectively than either the extract or GNPs alone (Figure 1).

GDF-9 Gene Expression

A dose-dependent increase in GDF-9 expression was observed particularly in the green gold nanoparticle (gGNP) 50 µg/mL group, showing the highest relative expression (fold change: ~3.4–3.5), followed by the GNP 50 µg/mL group. In contrast, high doses of *Achillea biebersteinii* extract (100 µg/mL) resulted in a significant downregulation of GDF-9 expression (fold change < 0.05), indicating a possible inhibitory effect at higher concentrations. The overall expression trend suggests that nanoparticle formulation enhances the stimulatory effect of the plant extract on GDF-9 transcription (Figure 2).

SOD Gene Expression

A significant increase in SOD expression was observed in the gGNP-treated groups at doses of 50 and 100 µg/mL compared to the control group ($p \leq 0.05$), while the GNP and AB extract groups showed no significant changes. These findings suggest that the green synthesis of nanoparticles using *Achillea biebersteinii* enhances antioxidant gene activation during folliculogenesis (Figure 3).

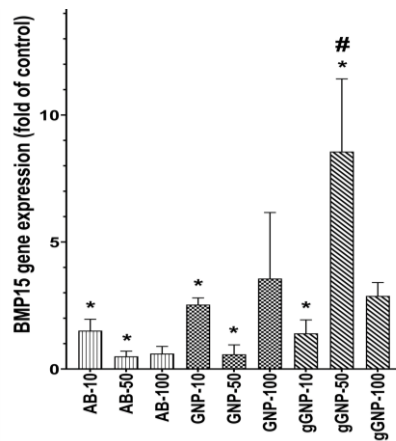


Figure 1. The level of BMP-15 gene expression in the different experimental groups. The values are expressed as the mean ± standard deviation. * Significant difference compared with the control group. # significant difference compared with the group treated with industrial gold nanoparticles at a dose of 50 µg/ml.

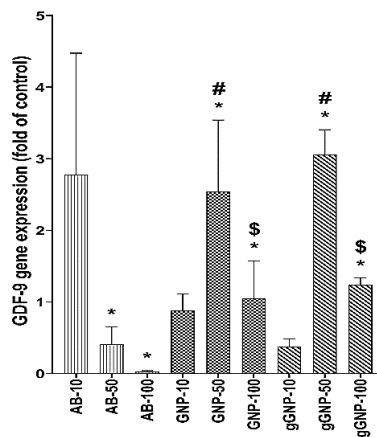


Figure 2. The level of GDF-9 gene expression in the different experimental groups. The values are expressed as the mean ± standard deviation. * Significant difference compared with the control group. # Significant difference compared with the AB group at a dose of 50 µg/ml. \$ Significant difference compared with the AB group at a dose of 100 µg/ml.

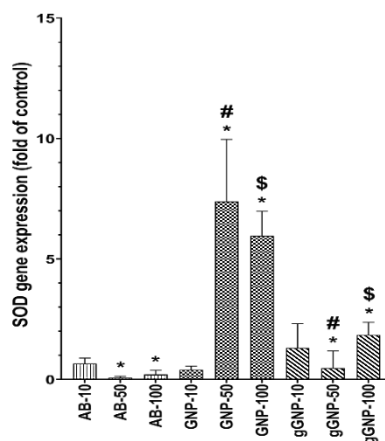


Figure 3. The level of SOD gene expression in different experimental groups. The values are expressed as the mean ± standard deviation. * Significant difference compared with the control group. # Significant difference compared with the AB group at a dose of 50 µg/ml. \$ Significant difference compared with the AB group at a dose of 100 µg/ml.

GPx Gene Expression

The expression of GPx gene increased significantly in the *Achillea biebersteinii* extract group in a dose-dependent manner. Although chemically synthesized GNPs showed limited or even suppressive effects on GPx expression, green-synthesized GNPs (gGNPs) notably enhanced GPx expression, particularly at 50 µg/mL. These findings indicate that the phytochemical components of the extract may play a crucial role in activating antioxidant defense pathways (Figure 4). In conclusion, our study provides evidence that both AB extract and GNPs can influence gene expression related to ovarian function. These findings offer a foundation for further research into the potential applications of AB extract and GNPs in reproductive health.

Follicle Counting Results

Primary Follicles

As shown in Table 2, the average number of primary follicles varied across treatment groups. No statistically significant differences ($p > 0.05$) were observed among the groups. Data are presented as mean \pm SEM.

Secondary Follicles

As shown in Table 3, the average number of secondary follicles varied across treatment groups. No statistically significant differences ($p > 0.05$) were observed among the groups. Data are presented as mean \pm SEM.

Graafian Follicles

As shown in Table 4, the average number of graafian follicles varied across treatment groups. No statistically significant differences ($p > 0.05$) were observed among the groups. Data are presented as mean \pm SEM.

Degenerated Follicles

As shown in Table 5, the average number of degenerated follicles varied across treatment groups. No statistically significant differences ($p > 0.05$) were observed among the groups. Data are presented as mean \pm SEM.

Histological study

Figure 5 shows tissue sections from the ovaries of the groups studied in this research. The figure clearly

illustrates the presence of several types of follicles, including primary follicles, secondary follicles, graafian follicles, and degenerated follicles. These follicles were identified, and in subsequent steps of the research, serial slices were prepared to count the follicles and to compare their numbers among the experimental groups.

The follicle counting results indicated that the GNP group at a dose of 10 µg/ml had the lowest number of primary, secondary, and graafian follicles compared to the other groups. Additionally, across all three doses, the GNP group demonstrated the highest number of degenerated follicles relative to the other groups. It is essential to emphasize that despite these observations, no statistically significant differences were observed, as detailed data are not shown.

The antrum diameter of secondary and Graafian follicles was measured in different treatment groups, including Control, *Achillea* extract, gold nanoparticles, and green synthesized nanoparticles at doses of 10, 50, and 100 mg.

For secondary follicles, no significant difference in antrum diameter was observed among groups at 10 mg and 50 mg doses ($p > 0.05$). However, at the 100 mg dose, a significant difference was detected ($F = 5.98$, $p = 0.020$). Post-hoc Tukey's test indicated a significant increase in antrum diameter in the green nanoparticle group compared to the gold nanoparticle group ($p < 0.05$). In Graafian follicles, no significant differences in antrum diameter were found among groups at any dose ($p > 0.05$). Tables 6 and 7 summarize the statistical distribution of antrum diameter measurements in secondary and Graafian follicles, respectively.

Statistical Analysis

All statistical analyses were performed using GraphPad Prism version 8. Data distribution was first assessed using the Shapiro–Wilk normality test. For multiple group comparisons, one-way ANOVA was conducted, followed by Tukey's multiple comparison test to identify specific group differences. Results are presented as mean \pm standard error of the mean (SEM). A p -value of ≤ 0.05 was considered statistically significant. The sample size for each group was $n = 6$, and each experiment was repeated independently at least three times. All graphs and statistical outputs were generated directly from GraphPad Prism.

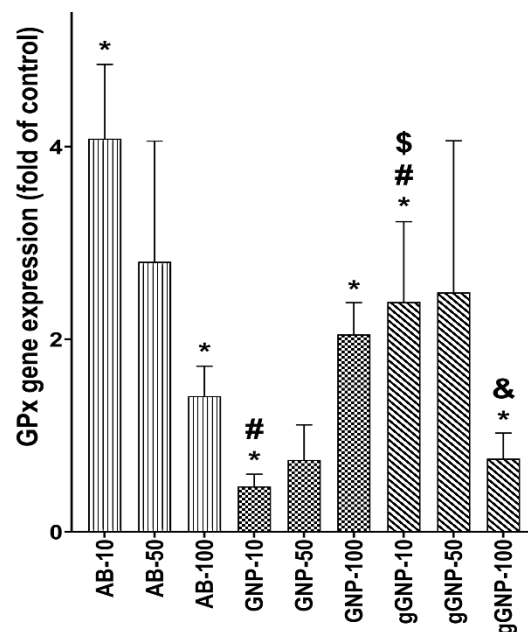


Figure 4. The level of GPx gene expression in different experimental groups. The values are expressed as the mean \pm standard deviation. * Significant difference compared with the control group. # Significant difference compared with the AB group at a dose of 10 μ g/ml. \$ Significant difference compared with the GNP group at a dose of 10 μ g/ml. & Significant difference compared with the GNP group at a dose of 100 μ g/ml.

Table 2. Statistical distribution of primary follicles data across groups

Group	Primary Follicles (Mean)	Primary Follicles (SEM)	Significance (p)
AB_10	9.0	1.0	ns
AB_100	10.0	0.0	ns
AB_50	6.5	0.5	ns
Control	11.5	0.5	ns
GNP_10	5.5	0.5	ns
GNP_100	9.5	0.5	ns
GNP_50	8.5	1.5	ns
gGNP_10	8.5	0.5	ns
gGNP_100	11.0	2.0	ns
gGNP_50	10.0	0.0	ns

Table 3. Statistical distribution of secondary follicles data across groups

Group	Secondary Follicles (Mean)	Secondary Follicles (SEM)	Significance (p)
AB_10	7.0	1.0	ns
AB_100	7.0	1.0	ns
AB_50	7.5	2.5	ns
Control	10.0	1.0	ns
GNP_10	6.5	1.5	ns
GNP_100	10.5	0.5	ns
GNP_50	8.0	0.0	ns
gGNP_10	11.5	0.5	ns

gGNP_100	12.5	2.5	ns
gGNP_50	11.0	1.0	ns

Table 4. Statistical distribution of graafian follicles data across groups

Group	Graafian Follicles (Mean)	Graafian Follicles (SEM)	Significance (p)
AB_10	9.0	3.0	ns
AB_100	9.0	1.0	ns
AB_50	8.5	2.5	ns
Control	13.0	1.0	ns
GNP_10	5.5	0.5	ns
GNP_100	9.0	1.0	ns
GNP_50	7.0	1.0	ns
gGNP_10	13.5	0.5	ns
gGNP_100	13.5	0.5	ns
gGNP_50	14.0	0.0	ns

Table 5. Statistical distribution of degenerated follicles data across groups

Group	Degenerated Follicles (Mean)	Degenerated Follicles (SEM)	Significance (p)
AB_10	6.5	1.5	ns
AB_100	3.0	0.0	ns
AB_50	5.5	0.5	ns
Control	2.5	0.5	ns
GNP_10	7.0	1.0	ns
GNP_100	7.5	0.5	ns
GNP_50	6.5	0.5	ns
gGNP_10	4.5	0.5	ns
gGNP_100	4.5	0.5	ns
gGNP_50	3.0	0.0	ns

Table 6. Statistical distribution of the antrum diameter in secondary follicles in different groups

Group	Dose (mg)	Mean Antrum Diameter (μm)	Standard Deviation (SD)
Control	10	–	–
AB	10	49.50	27.08
GNP	10	42.00	9.76
gGNP	10	45.17	18.67
Control	50	–	–
AB	50	35.60	14.36
GNP	50	32.50	17.68
gGNP	50	31.83	16.03
Control	100	–	–
AB	100	37.60	12.18
GNP	100	21.67	2.89
gGNP	100	61.60	22.90

ANOVA results: $F = 5.98$, $p = 0.020$ (significant difference at 100 mg dose). Post-hoc Tukey test: Significant difference between Green Nanoparticles and Gold Nanoparticles groups ($p < 0.05$)

Table 7. Statistical distribution of antrum diameter in Graafian follicles in different groups

Group	Dose (mg)	Mean Antrum Diameter (μm)	Standard Deviation (SD)
Control	10	80.33	19.40
AB	10	74.40	20.12
GNP	10	60.00	16.08

Group	Dose (mg)	Mean Antrum Diameter (μm)	Standard Deviation (SD)
gGNP	10	95.33	38.56
Control	50	80.33	19.40
AB	50	60.33	14.71
GNP	50	35.00	5.00
gGNP	50	68.17	29.94
Control	100	80.33	19.40
AB	100	82.50	51.92
GNP	100	26.67	11.55
gGNP	100	99.50	31.48

ANOVA results: No significant differences were observed among groups at any dose ($p > 0.05$)

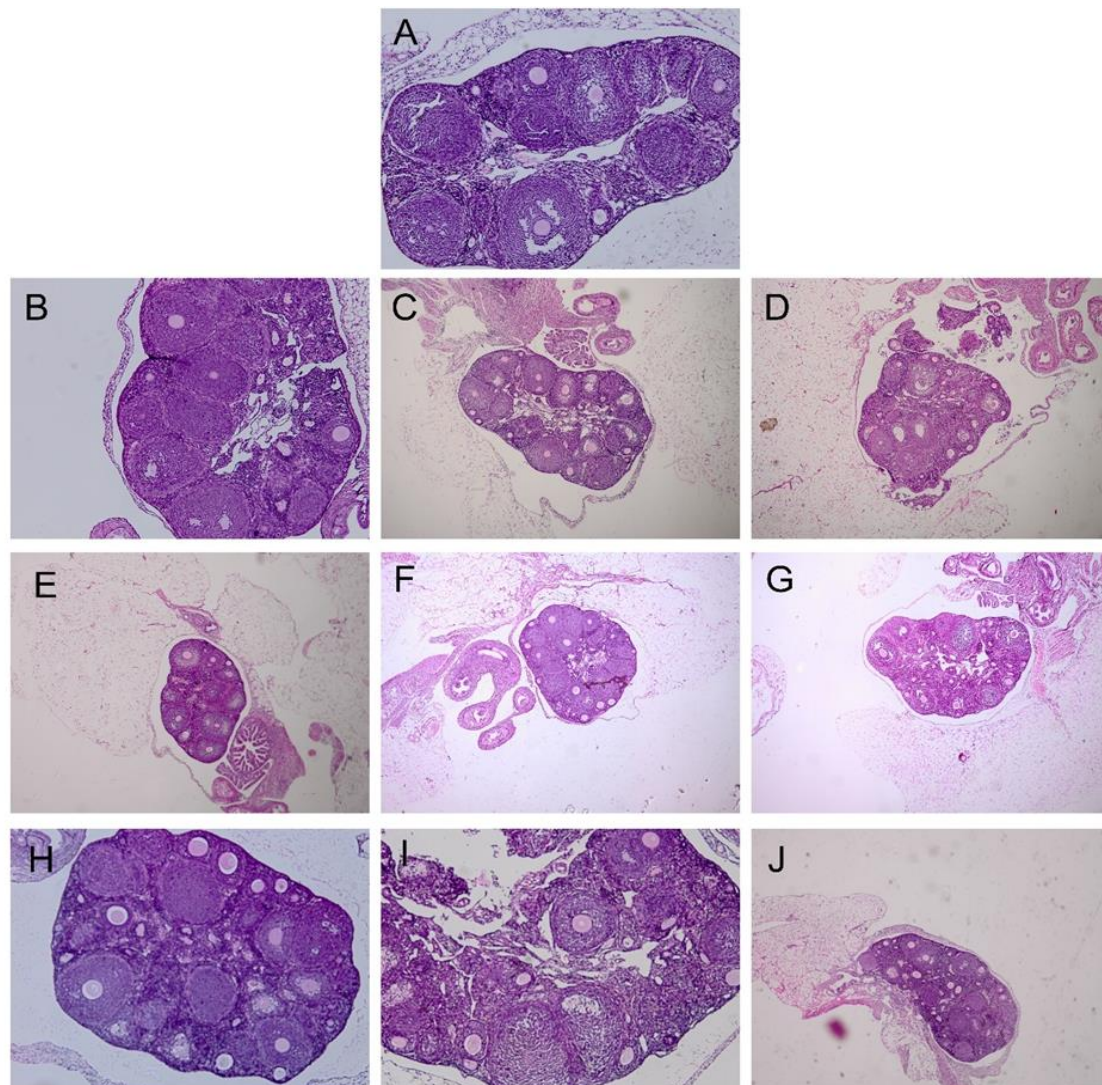


Figure 5. Optical photomicrograph of ovarian tissue. Hematoxylin and eosin staining was used to visualize the tissue structures. These images show sections of the ovaries from the control group (A); the AB group treated with 10 $\mu\text{g/ml}$ AB (B), 50 $\mu\text{g/ml}$ AB (C), and 100 $\mu\text{g/ml}$ AB (D); the DNP group treated with 10 $\mu\text{g/ml}$ AB (E), 50 $\mu\text{g/ml}$ AB (F), and 100 $\mu\text{g/ml}$ AB (G); and the gGNP group treated with 10 $\mu\text{g/ml}$ AB (H), 50

µg/ml AB (I), and 100 µg/ml AB (J). Primary, secondary, graafian and degenerated follicles were identified. Magnification: X 4.

Discussion

P Preantral follicles (PFs) are defined by the presence of oocytes surrounded by a single layer of squamous granulosa cells. These follicles initiate meiosis but remain arrested until fertilization. During the primary follicle stage, proliferation of granulosa cells establishes a multilayered structure essential for oocyte support and follicular growth. As follicles progress to the secondary stage, an antrum forms within the granulosa layer, and oocytes become centrally located following the first meiotic division. Follicular growth may be disrupted by toxic agents or enhanced by regulatory factors, which can accelerate oocyte maturation(23).

Previous studies have demonstrated that chemically synthesized gold nanoparticles (GNPs), even when coated with biocompatible agents like Bovine Serum Albumin (BSA), show minimal or inconsistent effects on PF maturation and granulosa proliferation (24). Some have even reported cytotoxicity to ovarian granulosa cells. In contrast, natural bioactive compounds—such as plant extracts—have shown promise in supporting follicular development(25). Our findings reveal that green-synthesized gold nanoparticles (gGNPs) using *Achillea biebersteinii* extract significantly enhanced the antrum diameter in secondary follicles compared to GNPs at the same concentration (100 µg/mL). However, in grafted follicles, no significant differences in antrum diameter were observed among groups. These results suggest that the phytochemical composition of the AB extract plays a role in promoting folliculogenesis—likely through antioxidant and signaling-modulatory properties. (26).

Toxicological analysis indicated that GNPs caused greater follicular atresia and reduction in follicle size, while gGNPs reduced these adverse effects. FTIR results support the presence of functional groups from the AB extract on the nanoparticle surface, which may underlie this improved biocompatibility(27).

From a gene expression perspective, the upregulation of BMP-15 and GDF-9 in gGNP-treated groups supports the hypothesis that green-synthesized nanoparticles may indirectly modulate the TGF-

β/SMAD pathway, given that these genes are well-known downstream targets. While we did not directly assess SMAD phosphorylation or nuclear translocation due to experimental limitations, our findings suggest functional activation of this signaling axis, warranting future investigation.(28).

Additionally, elevated levels of SOD and GPx, particularly in gGNP-treated groups, suggest that the phytochemicals in AB extract enhance antioxidant gene expression. While AB alone showed modest effects, the gGNP formulation amplified this response. This is consistent with prior studies reporting oxidative damage by metallic nanoparticles and the protective role of plant-derived antioxidants. These findings are consistent with prior studies reporting the antioxidant and anti-inflammatory properties of *Achillea biebersteinii* extract(29).It is important to acknowledge a key limitation of this study: direct mechanistic evaluations, such as SMAD pathway assays, ROS quantification, or nanoparticle uptake tracking, were not within the scope of this project (30).

Due to technical and resource constraints—particularly the complexity of the ovarian graft model in mice—this experiment cannot be feasibly repeated or extended. We have clearly stated this limitation in the revised manuscript and proposed these directions for future studies.

This study has several limitations. First, the number of animals per group was limited, which may have affected the statistical power of some comparisons. Second, due to technical and financial constraints, we were unable to perform direct mechanistic assays, such as SMAD protein phosphorylation, ROS quantification, or nanoparticle uptake in ovarian tissue. Third, we assessed only a limited number of gene targets, and broader transcriptomic profiling could provide deeper insights. Moreover, the complexity of the ovarian graft model limited our ability to replicate or extend the experiments further.

Despite this, we believe the present study provides novel insights by being the first to demonstrate the enhanced biological impact of *Achillea biebersteinii*-mediated gGNPs on oocyte-related gene expression and follicular parameters. The differential gene expression patterns and improved follicular

morphology provide a compelling foundation for further mechanistic exploration. Future studies should focus on elucidating the specific signaling pathways involved, particularly by performing SMAD phosphorylation assays and tracking the cellular uptake of gGNPs in ovarian tissues using imaging or labeling techniques. Additionally, oxidative stress quantification via ROS-specific markers and expanding the gene panel using transcriptomic or proteomic approaches would provide deeper mechanistic insights. Exploring the effects of different phytochemical profiles in Achillea species on nanoparticle efficacy may also reveal optimization strategies for green nanoparticle synthesis. In conclusion, our results suggest that the incorporation of AB extract in nanoparticle synthesis not only improves biocompatibility but also augments biological activity highlighting its potential as a safe and effective agent for reproductive tissue engineering and female fertility support.

Funding

This research was financed by Birjand University of Medical Sciences. The Ethics Committee of BUMS approved the investigations.

References

1. Fountas S, Petinaki E, Bolaris S, et al. The roles of GDF-9, BMP-15, BMP-4 and EMMPRIN in folliculogenesis and in vitro fertilization. *J. Clin. Med.* 2024;13(13):3775.
2. Crespo D, Fjellidal PG, Hansen TJ, et al. Loss of bmp15 function in the seasonal spawner Atlantic salmon results in ovulatory failure. *FASEB J.* 2024;38(14):e23837.
3. Otsuka F, McTavish KJ, Shimasaki S. Integral role of GDF- 9 and BMP- 15 in ovarian function. *Mol. Reprod. Dev.* 2011;78(1):9-21.
4. Sanfins A, Rodrigues P, Albertini DF. GDF-9 and BMP-15 direct the follicle symphony. *J. Assist. Reprod. Genet.* 2018;35(10):1741-50.
5. Hanrahan JP, Gregan SM, Mulsant P, et al. Mutations in the genes for oocyte-derived growth factors GDF9 and BMP15 are associated with both increased ovulation rate and sterility in Cambridge and Belclare sheep (*Ovis aries*). *Biol. Reprod.* 2004;70(4):900-9.
6. Hariyanto NI, Yo EC, Wanandi SI. Regulation and Signaling of TGF- β Autoinduction. *Int. J. Mol. Cell. Med.* 2022;10(4):234.
7. Baba AB, Rah B, Bhat GR, et al. Transforming growth factor-beta (TGF- β) signaling in cancer-A betrayal within. *Front. Pharmacol.* 2022;13:791272.
8. Singh A. Effects of BMP15 and GDF9 on Ovine Oocytes in an In Vitro Maturation System: Open Access Te Herenga Waka-Victoria University of Wellington; 2020.
9. Chen H, Liu C, Jiang H, et al. Regulatory role of miRNA-375 in expression of BMP15/GDF9 receptors and its effect on proliferation and apoptosis of bovine cumulus cells. *Cell. Physiol. Biochem.* 2017;41(2):439-50.
10. Chen Y, Yang J, Zhang L. The impact of follicular fluid oxidative stress levels on the outcomes of assisted reproductive therapy. *Antioxidants.* 2023;12(12):2117.
11. Sasaki H, Hamatani T, Kamijo S, et al. Impact of oxidative stress on age-associated decline in oocyte developmental competence. *Front. Endocrinol.* 2019;10:811.
12. Shi Y-Q, Zhu X-T, Zhang S-N, et al. Premature ovarian insufficiency: a review on the role of oxidative stress and the application of antioxidants. *Front. Endocrinol.* 2023;14:1172481.
13. Smits A. Opportunities for improvement of oocyte quality in metabolically compromised conditions: from fundamental discoveries in the well until the development of preconception care strategies in an obese mouse model: University of Antwerp; 2022.
14. Yoshida S, Hiyoshi K, Ichinose T, et al. Effect of nanoparticles on the male reproductive system of mice. *Int. J. Androl.* 2009;32(4):337-42.
15. Daraee H, Eatemadi A, Abbasi E, et al. Application of gold nanoparticles in biomedical and drug delivery. *Artif. Cells Nanomed. Biotechnol.* 2016;44(1):410-22.
16. Adeyemi JO, Oriola AO, Onwudiwe DC, et al. Plant extracts mediated metal-based nanoparticles: synthesis and biological applications. *Biomolecules.* 2022;12(5):627.
17. Mikhailova EO. Gold nanoparticles: Biosynthesis and potential of biomedical application. *J. Funct. Biomater.* 2021;12(4):70.
18. Mirahmadi SF, Norouzi R. Chemical composition, phenolic content, free radical scavenging and

- antifungal activities of *Achillea biebersteinii*. *Food Biosci.* 2017;18:53-9.
19. Ashique S, Mukherjee T, Mohanty S, et al. Blueberries in focus: Exploring the phytochemical potentials and therapeutic applications. — *J. Agric. Food Res.* 2024;18:101300.
 20. Platzer M, Kiese S, Tybussek T, et al. Radical scavenging mechanisms of phenolic compounds: A quantitative structure-property relationship (QSPR) study. *Front. Nutr.* 2022;9:882458.
 21. Abdollahi MR, Afkhami-Ardakani M, Saadatfar Z, et al. The effect of gold nanoparticles synthesized with *Achillea biebersteinii* on gene expression in Cultured preantral Follicles derived from NMRI mice ovary. *Gene Rep.* 2022;26:101449.
 22. Abdollahi M, Baharara J, Shahrokhadi K, et al. The effect of green gold nanoparticles synthesized with the *Achillea millefolium* extract on the morphometric and developmental indices of preantral follicles in immature NMRI mice. *Thrita.* 2020;9(2).
 23. Qu J, Wang Q, Sun X, et al. The environment and female reproduction: Potential mechanism of cadmium poisoning to the growth and development of ovarian follicle. *Ecotoxicol. Environ. Saf.* 2022;244:114029.
 24. Taylor U, Tiedemann D, Rehbock C, et al. Influence of gold, silver and gold–silver alloy nanoparticles on germ cell function and embryo development. *Beilstein J. Nanotechnol.* 2015;6(1):651-64.
 25. Barathi Seetharaman AC, Santosh W, Vasantharekha R. 12 Potential Health Benefits of Phytochemical Compounds on Endocrine Disruption and Female Reproductive Health. *Plant Biol. Transl. Med.* 2024:192.
 26. Rajabi-Toustani R, Motamedi-Mojdehi R, Mehr MR-A, et al. Effect of *Papaver rhoeas* L. extract on in vitro maturation of sheep oocytes. *Small Rumin. Res.* 2013;114(1):146-51.
 27. Mobaraki F, Momeni M, Yazdi MET, et al. Plant-derived synthesis and characterization of gold nanoparticles: Investigation of its antioxidant and anticancer activity against human testicular embryonic carcinoma stem cells. *Process Biochem.* 2021;111:167-77.
 28. Siddiqi NJ, Abdelhalim MAK, El-Ansary AK, et al. Identification of potential biomarkers of gold nanoparticle toxicity in rat brains. *J. Neuroinflammation.* 2012;9:1-7.
 29. BarathManiKanth S, Kalishwaralal K, Sriram M, et al. Anti-oxidant effect of gold nanoparticles restrains hyperglycemic conditions in diabetic mice. *J. Nanobiotechnol.* 2010;8(1):1-15.
 30. Ding Y, Wang H, Wang Y, et al. Co-delivery of luteolin and TGF- β 1 plasmids with ROS-responsive virus-inspired nanoparticles for microenvironment regulation and chemo-gene therapy of intervertebral disc degeneration. *Nano Res.* 2022;15(9):8214-27.